Changes in xylem conducting capacity and water storage across species: how can variable air content of xylem cells affect sap flow?

A.J. McElrone[1,2,a], J.M. Earles[3], T.M. Knipfer[2], C.P. Albuquerque[2], C.R. Brodersen[3] and I.F. Cuneo[4]

[1]USDA-ARS, Crops Pathology and Genetics Research Unit, Davis, California, USA; [2]Department of Viticulture and Enology, University of California, Davis, California, USA; [3]School of Forestry & Environmental Studies, Yale University, New Haven, Connecticut, USA; [4]Escuela de Agronomía, Pontificia Universidad Católica de Valparaíso, Quillota, Chile.

Abstract

Sap flow sensors and other techniques are commonly used across species and plant organs to quantify water use and storage, detect stress, and evaluate the contribution of various tissues to plant/organ water balance. Sap flow methods often rely upon modelling or assumptions about how heat delivered by the sap flow sensors is partitioned into convection and conduction into active sapwood xylem and surrounding tissues. Dynamic changes in tissue water content over space and time can impact the interpretation of plant and organ water use and how various compartments contribute to an integrated response to plant stress. Here, we first summarize results from a variety of studies that used a combination of synchrotron-based X-ray microCT and MRI imaging to demonstrate how water content of various organs and xylem cell types can change temporally and how the spatial distribution of air-filled tissue may impact patterns of sap flow within the xylem network. Results from visualization techniques were compared to that from traditional hydraulic and sap flow methods to illustrate potential discrepancies particularly when comparing data from excised stems versus intact plants. Using a spatially explicit model, we demonstrate how changes in the water content of various cell types can impact resulting interpretation of sensor output. Implications for the interpretation of sap flow and other sensor data based on these results is discussed.

Keywords: thermal dissipation probes, thermal conductivity, tissue moisture content, heat pulse sensors, capacitance, water storage, xylem embolism, finite element modelling

INTRODUCTION

Non-invasive visualization techniques, such as magnetic resonance imaging (MRI) and x-ray micro-computed tomography (microCT), are being used more frequently to study plant water transport in vivo (e.g., Holbrook et al., 2001; Kaufmann et al., 2009; Brodersen et al., 2010; Knipfer et al., 2015, 2016; Choat et al., 2015). These techniques have provided new insights into the structure and function of plant hydraulic networks that could impact our understanding and interpretation of datasets captured with sap flow methods and other plant hydraulic and water relations techniques. Lee et al. (2013) recently modelled sap flow in three-dimensional xylem networks derived from microCT, and found that flow in 27% of the vessels was oriented in the direction opposite the bulk flow in the xylem network under normal transpirational conditions. This example highlights that efforts should be made moving forward to integrate findings across scales to improve sap flow methods and our understanding of data generated from these techniques.

Non-invasive techniques have also raised doubts about some commonly held paradigms in plant hydraulics. For example, while xylem embolism plays a critical role in

[a]E-mail: ajmcelrone@ucdavis.edu

plant mortality under conditions of severe water stress (e.g., Choat, 2013), direct microCT visualizations across numerous species and organs show that minimal cavitation occurs in xylem conduits under mild to moderate water stress (i.e., Scoffoni et al., 2017a, b; Cuneo et al., 2016; Hochberg et al., 2016; Choat et al., 2010; Brodersen et al., 2013). These findings suggest that daily cycles of embolism formation and repair are not commonplace (Cochard and Delzon, 2013). Furthermore, Knipfer et al. (2017) found that refilling of both capillary water storage (i.e., fibers) and vessels occurs rarely or never under in-vivo conditions over two time scales, 24 h and 3 weeks, for *Laurus nobilis* saplings, but patterns of overnight sap flow in trees have been attributed to diurnal cycles of storage tissue discharge and recharge (Goldstein et al., 1998). Knipfer et al. (2017) also found that fibers refill when excised samples are attached to a water source, which impact sap flow sensor calibrations conducted on excised plant segments.

Visualization techniques and modelling provide an opportunity to evaluate whether dynamic changes in xylem tissue water content (i.e., fiber and vessels) occur on a daily basis across plant species, which can improve sap flow methods and data interpretation for intact plants. This could also help to resolve whether artefactual refilling and internal hydraulic redistribution that occurs in excised samples (e.g., Knipfer et al., 2016) impacts sap flow sensor calibrations and whether dye infiltrations, which are commonly used for sensor calibration and translation of flow velocities to values of volumetric water use, accurately represent sap flow for intact plants.

This manuscript represents a thought exercise based on what we have learned about xylem functioning from advanced visualization techniques in recent years, and how it potentially impacts the interpretation of our sap flow and other sensors data. We show varied examples of xylem tissue water content in single stems and across species, and then use finite element modelling to demonstrate effects on sap flow sensor output, which was shown to vary dramatically depending on the hydration status of the tissues surrounding sap flow sensor heating elements.

MATERIAL AND METHODS

Plant materials used in the experiments were grown in a greenhouse facility at the University of California, Davis. *Laurus nobilis* and *Acer rubrum* saplings (~60 cm height) were obtained from commercial nurseries. *Vitis vinifera* 'Cabernet Sauvignon' were obtained from two sources: 1) own-rooted cuttings propagated in our greenhouse; and 2) UberVines (~80 cm height) obtained from Duarte Nursery, Hughson, CA. The bench grafted UberVine (magnum) utilizes an extra-long rootstock (110R) cane, so it can be tied directly to the training wire when planted. The cane is cut in the air during the grafting process and thus embolizes any existing xylem vessels in these vines. Thus the majority of xylem in our scanned cross-sections were air-filled at the time of our microCT scanning (Figure 1), but new xylem had started to grow on the outer edge of the stem.

Plants were grown in either 4- or 6-inch diameter plastic pots filled with soil mix (equal parts of peat moss, composted bark, sand and perlite) and maintained for ~6 weeks under typical summer greenhouse conditions (approximated day/night temperature of 25/8°C, photoperiod of 15/9 h, relative humidity of 35%). Plants were irrigated daily with water supplemented with macro- and micro-nutrients (similar to Knipfer et al., 2015).

Plant material was scanned at the X-ray micro-tomography facility (Beamline 8.3.2) at the Lawrence Berkley National Laboratory. Saplings were transported by car to the Advanced Light Source (ALS, Lawrence Berkeley National Lab, Berkeley, CA) less than 4 h prior to analysis. For visualization of stem tissue, the potted sapling was placed in an aluminum cage and was scanned over a small axial distance on the stems. For some vines the stem portion scanned on the intact plants were excised, dried at 40°C and rescanned ~24 h later (Figure 1). Stems were scanned in a 21 keV synchrotron X-ray beam using a continuous tomography setting yielding 1025 two-dimensional longitudinal images (resolution of 3.22 μm $pixel^{-1}$) that were captured on a CMOS camera (PCO.edge; PCO, Kehlheim, Germany) at 350 ms exposure time. Acquired raw images were reconstructed into transverse images using a custom software plugin for Fiji image-processing software (www.fiji.sc, ImageJ) that

used Octopus software (ver. 8.3; National Institutes for Nuclear Science, Ghent University, Ghent, Belgium) in the background (Knipfer et al., 2016). Longitudinal images were generated using the slice tool in the software AVIZO (ver. 6.2; Visualization Sciences Group/FEI, Hillsboro, Oregon, USA).

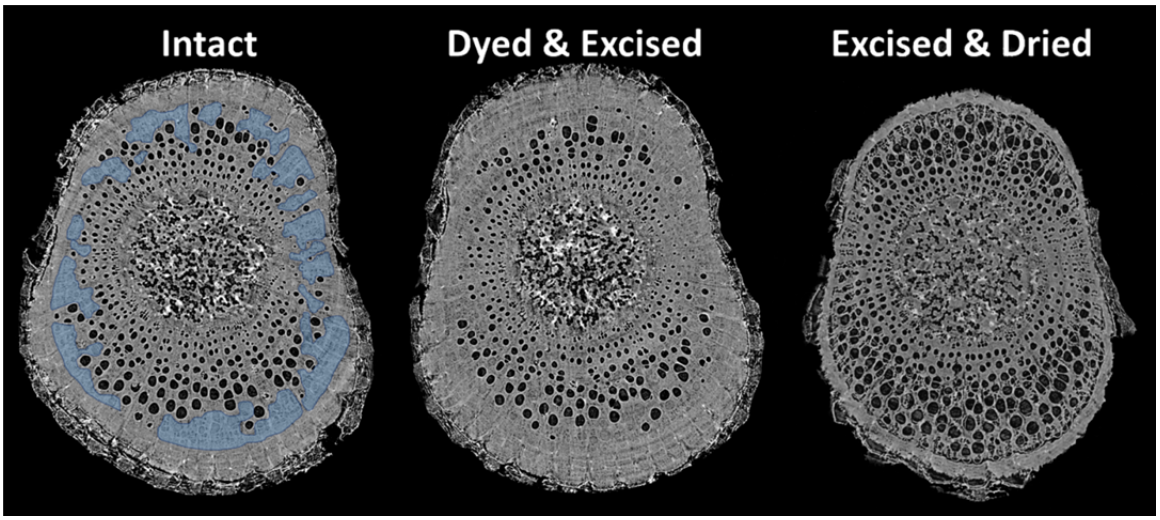

Figure 1. Comparison of intact, excised, and dried states for a grapevine stem captured using microCT at the same axial location on the same plant. The blue area for the first image highlights the fluid filled vessels in the intact state. After being scanned, dye infiltration was performed on an actively transpiring shoot at midday while the base of the stem was submerged in the dye solution. Image on the right shows the stem fully embolized after being dried.

Dye infiltrations were conducted on grapevines to assess the conductive sapwood area after microCT scanning of the intact plants using a method similar to that described in Pearsall et al. (2014). The vines were maintained outside the ALS facility placed in the sunlight prior to the intact scan and during the dye infiltration. Vines stems were submerged in a crystal violet dye solution, then the segment was cut with sharp pruning shears. The cut end was then quickly recut with a fresh razor blade to limit vessel clogging, and the bottom of the stem was held submerged under the dye until it appeared in the leaf material (between 30-60 min). Transpiration rates for these vines were confirmed just prior to dye infiltration by measuring weight loss from the plant, where the soil and the pot were sealed in double plastic bags to prevent evaporation. These data were used to calculate sap flow velocity in the remaining vessels from the intact plant scan vs. the dried sample.

RESULTS AND DISCUSSION

The dye infiltration experiment was performed on transpiring grapevines that were cut while the stem was submerged in dye solution. This was effective in identifying the active sap wood area, this is a standard method for assessing active sapwood area for sap flow techniques (e.g., Pearsall et al., 2014). MicroCT scans of a grapevine shoot before and after the excision showed that similar numbers of vessels were fluid filled before and after the infiltration (Figure 1, left and middle images), and the active xylem area composed of water-filled vessels was limited to the very outer edge (i.e., the youngest xylem). A scan of the dried sample (Figure 1, right) revealed that all the fluid-filled vessels in the dyed area emptied upon drying suggesting these were filled with water in the intact plant. The grapevines (UberVines) were actively transpiring at the time of the dye infiltration experiment. On average, these vines were transpiring at a rate of 4.34 g H_2O h^{-1} during the period just prior to dye infiltration. In comparison to alternative dye infiltration methods, this method of dye infiltration is preferred to dye infiltration on an excised stem segment with two open ends (i.e., cut at the base of the stem and just below the leaves, resulting in a single segment). If

the excised segment is shorter than the longest vessels, this can result in numerous vessels opened at both ends of the segment that would create preferential flow paths and dominate dye infiltration and conductivity measurements, which may not represent the status of the intact xylem network.

Higher resolution microCT scans better illustrate the thin active band of water filled vessels in the imaged grapevine plant (Figure 2) and correspond well with the dye infiltration in the outer most portion of the xylem nearest the cambium. Interestingly, the older xylem was always embolized (i.e., did not refill) despite these plants being maintained in a well-watered state in the greenhouses during 6 weeks prior to the experiment, enough time for embolism refilling in grapevines (Knipfer et al., 2015). Despite the fact that grapevines can refill embolized conduits (Holbrook et al., 2001; Brodersen et al., 2010; Knipfer et al., 2015), these older vessels remained air-filled, and recovery of xylem conductivity was associated with growth of new vessels upon reconnection of the vascular tissue in the graft. These images also illustrate the difficulties of placing insertion sap flow probes into the active sap wood for plants like these and of accurately measuring the active sap wood area. Flow rates under such conditions would likely involve very few vessels, especially when accounting for wounding effects associated with needle insertion, and could suffer from heat being dissipated differentially in parts of the cross section with different vessel embolism status.

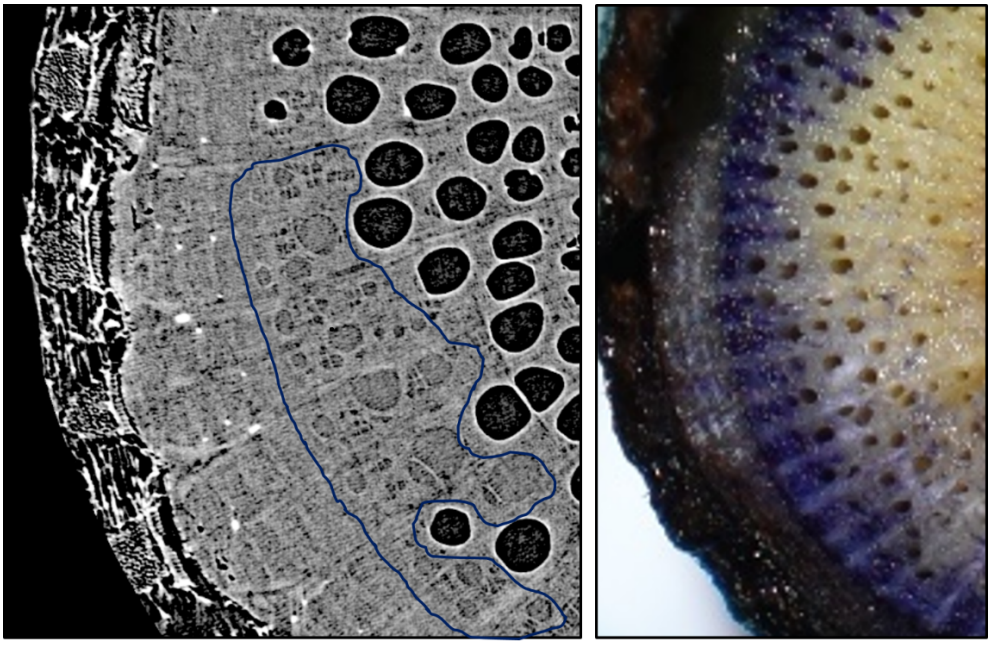

Figure 2. Example of the thin active cross-sectional area of an UberVine grafted grapevine examined with microCT (left panel) and excised dyed stem (right panel). The active (water-filled) vessels in the microCT image are in the region outlined in blue. The very shallow active cross-sectional area in these two-year-old plants results from all of the previous year's xylem becoming inactive when the scion was grafted onto the UberVine rootstock. This plant was actively transpiring at the time of dyeing, and the older xylem remained in an empty state (i.e., the plant is relying on a very thin band of active xylem closest to the cambium for transporting water to transpiring foliage).

MicroCT scans collected across several species revealed that fiber lumen content (i.e., water vs. air) can differ across species and in the same plant (Figures 3 and 4). The microCT image of *Vitis vinifera* showed embolized vessels, while the surrounding xylem tissue (fibers and parenchyma) remained water-filled (Figure 3, left); grapevine fibers, like other lianas,

are living at maturity and contain a viable cell membrane (Knipfer et al., 2016), thus can remain water-filled even under severe stress. The only time we have seen fibers empty in grapevines is when plants are infected with fungal pathogens that target the living fibers and parenchyma cells (Czemmel et al., 2015; McElrone, pers. observ.). It should be noted that tracheids (imperforate tracheary elements) are also common in many liana species, including *Vitis vinifera*, and are characterized by distinctly bordered pits with intact pit membranes that are similar to vessel-vessel pit membranes. On the other hand, fibers do not contribute to axial transport and do not show distinctly bordered pits. Fibers can be filled with air or capillary water or remain living for a long time, which would also give these the impression of being water-filled in microCT scans. Often tracheids and fibers occur together, which makes the cell diversity rather complex, and macerations combined with tangential and radial sections are useful to observe imperforate tracheary elements in detail.

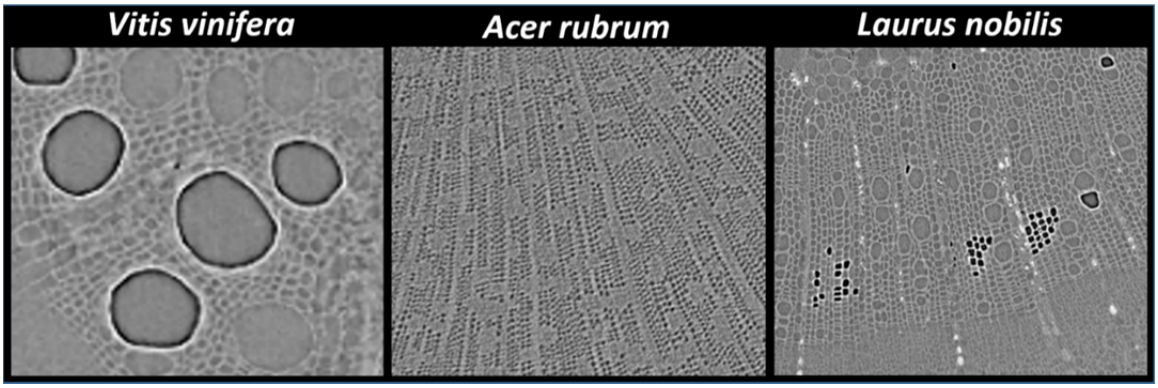

Figure 3. Transverse microCT images for three species (grapevine – left panel; red maple – middle panel; and bay laurel – right panel) under water stress demonstrating the variability in tissue water content that can exist. Fibers in *V. vinifera* are living at maturity and remain water-filled unless this tissue is infected with a fungal pathogen. The fibers in *Acer rubrum* for this sample emptied under mild drought stress and long before embolism formation. *Laurus nobilis* exhibits patterns where the vessels and fibers can empty at similar stress leaves. The fibers in the latter two species are dead at maturity.

In contrast to grapevines, the microCT image of *Acer rubrum* exhibited empty fibers in the mature xylem while the ray parenchyma was hydrated, and all xylem vessels filled with water (Figure 3, middle), and *Laurus nobilis* showed mostly water-filled vessels and fibers, but some patches of air-filled fibers (Figure 3, right). A scan of an additional *L. nobilis* plant revealed this pattern could be quite variable even within the same plant (Figure 4). Four possible combinations with xylem hydration status were seen in these plants: 1) water-filled vessels and fibers located close the cambium (blue box in Figure 4, right, FV-FF); 2) water-filled vessels and empty (i.e., air-filled) fibers (green box in Figure 4, right, FV-EF); 3) empty vessels and water-filled fibers (grey box in Figure 4, right, EV-FF); and 4) empty vessels and empty fibers (black box in Figure 4, right, EV-EF). Such patterns within a single plant could cause significant problems with sap flow methods given that heat dissipation would vary dramatically along the length of an insertion probe inserted into this tissue. For example, heat conductive properties of air and water vary considerably, and flow rates where vessels are functional, but fibers are either water or air-filled would introduce errors into the apparent versus actual flow rates at each point.

To test this idea, we used a simplified finite element model where filled and water conducting vessels were surrounded by either water- or air-filled fibers (Figure 5). Temperature trace outputs from this simulation were fed into the heat ratio method (Burgess et al., 2001) algorithms and revealed that apparent velocities were significantly higher when fibers were air-filled compared to the water-filled state (Figure 6). Under both

low and high flow conditions (i.e., 5 and 50 cm h^{-1}, respectively), the apparent flow rates were dramatically higher when conducting vessels were surrounded by air-filled fibers (Figure 6).

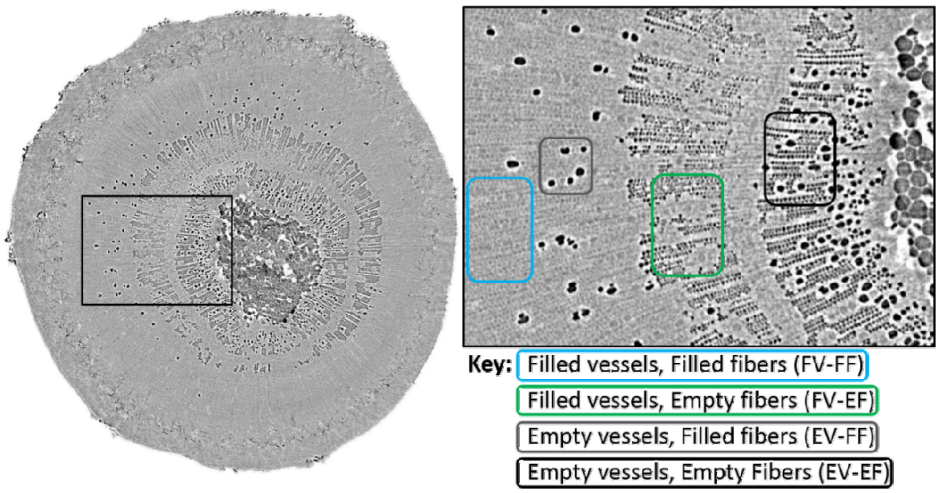

Figure 4. Example of an intact plant stem (*Laurus nobilis*) exhibiting xylem tissue with varied states of lumen filling. Varied states include water-filled vessels (FV), water-filled fibers (FF), empty vessels (EV), empty fibers (EF). Image was captured with synchrotron-based x-ray microCT at ALS on an intact potted plant. This figure illustrates that sensor placement, sensor output, and active cross-sectional area of such a stem would create difficulties in understanding the sap flow sensor output.

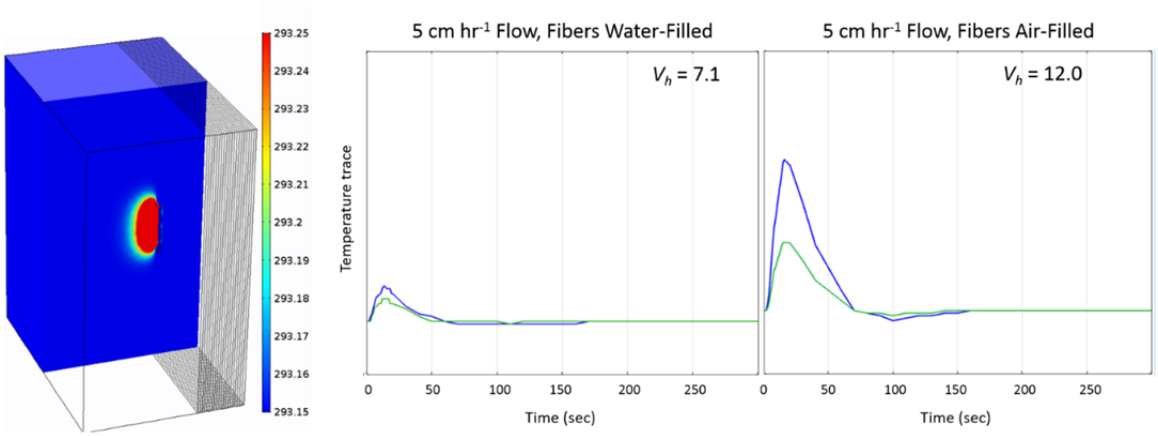

Figure 5. Illustration of the finite element model (left image) used to simulate heat dissipation away from a heater element and into the surrounding tissue via conductance and convection. Resulting temperature traces for the two fiber states under low flow conditions are presented (right panels) in a heat ratio method sap flow configuration. V_h is the resultant heat pulse velocity for this theoretical sensor.

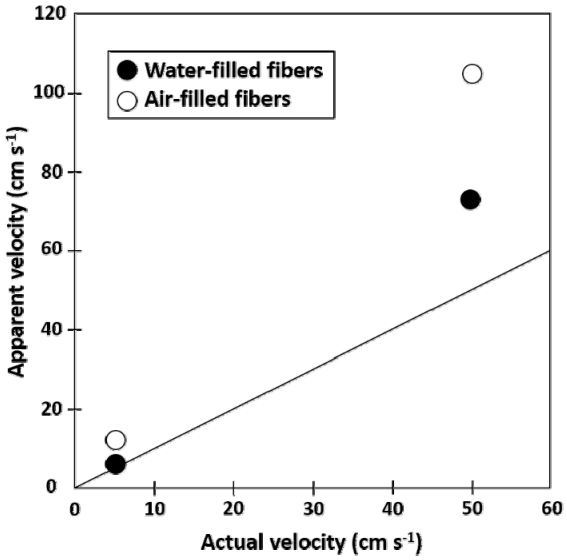

Figure 6. Apparent velocities versus the imposed actual velocities used to drive the FEM simulation compared to the 1:1 line (solid black line).

CONCLUSIONS

It is currently unknown how patterns of tissue hydration vary within plants and across species, and it is impossible to currently test this for installations under field conditions. Knipfer et al. (2017) recently showed that xylem fibers rarely refilled in intact plants, but fiber tissue refilled rapidly when the tissue was excised and attached to a water source. Such rehydration measurements are commonly used to infer details about tissue water storage capacity. Knipfer et al. (2016) also showed that water can be internally redistributed (i.e., moving out of vessels and into surrounding xylem cells) in excised grapevine stems attached to a water source. Given that calibrations of sap flow and other sensors are often conducted on excised samples in the lab, it is important to test whether xylem tissue hydration status is changing under these artificial conditions and to determine how this impacts our calibrations. Future sap flow technique developments would likely benefit from pairing with xylem network properties derived from non-invasive techniques like microCT. Samples from intact field plants may be able to be excised from flash frozen cross sections (thus maintaining their natural status) to assess hydration variability between xylem cell types in different parts of the cross-section.

ACKNOWLEDGEMENTS

AJM would like to thank the symposium organizers and ISHS for the invitation, opportunity, and financial support to present a keynote talk. Work presented in this talk was funded by the USDA-ARS Sustainable Viticulture CRIS (grant no. 5306-21220-004-00). The Advanced Light Source is supported by the Director, Office of Science, Office of Basic Energy Science, of the US Department of Energy under contract no. DE-AC02-05CH11231, The California Grapevine Rootstock Improvement Commission, and The American Vineyard Foundation. CPA thanks CAPES/Brazil and the UC Davis Department of Viticulture & Enology for financial support.

Literature cited

Brodersen, C.R., McElrone, A.J., Choat, B., Matthews, M.A., and Shackel, K.A. (2010). The dynamics of embolism repair in xylem: in vivo visualizations using high-resolution computed tomography. Plant Physiol. *154* (*3*), 1088–1095 https://doi.org/10.1104/pp.110.162396. PubMed

Brodersen, C.R., McElrone, A.J., Choat, B., Lee, E.F., Shackel, K.A., and Matthews, M.A. (2013). In vivo visualizations of drought-induced embolism spread in *Vitis vinifera.* Plant Physiol. *161* (*4*), 1820–1829 https://doi.org/10.1104/pp.112.212712. PubMed

Burgess, S.S.O., Adams, M.A., Turner, N.C., Beverly, C.R., Ong, C.K., Khan, A.A.H., and Bleby, T.M. (2001). An improved heat pulse method to measure low and reverse rates of sap flow in woody plants. Tree Physiol. *21* (*9*), 589–598 https://doi.org/10.1093/treephys/21.9.589. PubMed

Choat, B. (2013). Predicting thresholds of drought-induced mortality in woody plant species. Tree Physiol. *33* (*7*), 669–671 https://doi.org/10.1093/treephys/tpt046. PubMed

Choat, B., Drayton, W.M., Brodersen, C., Matthews, M.A., Shackel, K.A., Wada, H., and McElrone, A.J. (2010). Measurement of vulnerability to water stress-induced cavitation in grapevine: a comparison of four techniques applied to a long-vesseled species. Plant Cell Environ. *33* (*9*), 1502–1512. PubMed

Choat, B., Brodersen, C.R., and McElrone, A.J. (2015). Synchrotron X-ray microtomography of xylem embolism in *Sequoia sempervirens* saplings during cycles of drought and recovery. New Phytol. *205* (*3*), 1095–1105 https://doi.org/10.1111/nph.13110. PubMed

Cochard, H., and Delzon, S. (2013). Hydraulic failure and repair are not routine in trees. Ann. For. Sci. *70* (*7*), 659–661 https://doi.org/10.1007/s13595-013-0317-5.

Cuneo, I.F., Knipfer, T., Brodersen, C.R., and McElrone, A.J. (2016). Mechanical failure of fine root cortical cells initiates plant hydraulic decline during drought. Plant Physiol. *172* (*3*), 1669–1678 https://doi.org/10.1104/pp.16.00923. PubMed

Czemmel, S., Galarneau, E.R., Travadon, R., McElrone, A.J., Cramer, G.R., and Baumgartner, K. (2015). Genes expressed in grapevine leaves reveal latent wood infection by the fungal pathogen *Neofusicoccum parvum.* PLoS ONE *10* (*3*), e0121828 https://doi.org/10.1371/journal.pone.0121828. PubMed

Goldstein, G., Andrade, J.L., Meinzer, F.C., Holbrook, N.M., Cavelier, J., Jackson, P., and Celis, A. (1998). Stem water storage and diurnal patterns of water use in tropical forest canopy trees. Plant Cell Environ. *21* (*4*), 397–406 https://doi.org/10.1046/j.1365-3040.1998.00273.x.

Hochberg, U., Albuquerque, C., Rachmilevitch, S., Cochard, H., David-Schwartz, R., Brodersen, C.R., McElrone, A., and Windt, C.W. (2016). Grapevine petioles are more sensitive to drought induced embolism than stems: evidence from in vivo MRI and microCT observations of hydraulic vulnerability segmentation. Plant Cell Environ. *39*, 1886–1894 https://doi.org/10.1111/pce.12688. PubMed

Holbrook, N.M., Ahrens, E.T., Burns, M.J., and Zwieniecki, M.A. (2001). In vivo observation of cavitation and embolism repair using magnetic resonance imaging. Plant Physiol. *126* (*1*), 27–31 https://doi.org/10.1104/pp.126.1.27. PubMed

Kaufmann, I., Schulze-Till, T., Schneider, H.U., Zimmermann, U., Jakob, P., and Wegner, L.H. (2009). Functional repair of embolized vessels in maize roots after temporal drought stress, as demonstrated by magnetic resonance imaging. New Phytol. *184* (*1*), 245–256 https://doi.org/10.1111/j.1469-8137.2009.02919.x. PubMed

Knipfer, T., Eustis, A., Brodersen, C., Walker, A.M., and McElrone, A.J. (2015). Grapevine species from varied native habitats exhibit differences in embolism formation/repair associated with leaf gas exchange and root pressure. Plant Cell Environ. *38* (*8*), 1503–1513 https://doi.org/10.1111/pce.12497. PubMed

Knipfer, T., Cuneo, I.F., Brodersen, C.R., and McElrone, A.J. (2016). In-situ visualization of the dynamics in xylem embolism formation and removal in the absence of root pressure: a study on excised grapevine stems. Plant Physiol. *171* (*2*), 1024–1036. PubMed

Knipfer, T., Cuneo, I.F., Earles, J.M., Reyes, C., Brodersen, C.R., and McElrone, A.J. (2017). Storage compartments for capillary water refill in excised stems but rarely refill in intact woody plants (*Laurus nobilis*): visualization of tissue-specific dynamics using microCT imaging. Plant Physiol. *175*, 1649–1660 https://doi.org/10.1104/pp.17.01133. PubMed

Lee, E.F., Matthews, M.A., McElrone, A.J., Phillips, R.J., Shackel, K.A., and Brodersen, C.R. (2013). Analysis of HRCT-derived xylem network reveals reverse flow in some vessels. J. Theor. Biol. *333*, 146–155 https://doi.org/10.1016/j.jtbi.2013.05.021. PubMed

Pearsall, K., Williams, L.E., Castorani, S.E., Bleby, T.M., and McElrone, A.J. (2014). Evaluating the potential of a novel dual heat pulse sensor to measure volumetric water use in grapevines under a range of flow conditions. Funct. Plant Biol. *41* (*8*), 874–883 https://doi.org/10.1071/FP13156.

Scoffoni, C., Albuquerque, C., Brodersen, C.R., Townes, S.V., John, G.P., Bartlett, M.K., Buckley, T.N., McElrone, A.J., and Sack, L. (2017a). Outside-xylem vulnerability, not xylem embolism, controls leaf hydraulic decline during dehydration. Plant Physiol. *173* (*2*), 1197–1210 https://doi.org/10.1104/pp.16.01643. PubMed

Scoffoni, C., Albuquerque, C., Brodersen, C.R., Townes, S.V., John, G.P., Cochard, H., Buckley, T.N., McElrone, A.J., and Sack, L. (2017b). Leaf vein xylem conduit diameter influences susceptibility to embolism and hydraulic decline. New Phytol. *213* (*3*), 1076–1092 https://doi.org/10.1111/nph.14256. PubMed